A Review on Mutiphase Flows and Applications

Nouri Fatma Zohra

Mathematical Modeling and Numerical Simulation Research Laboratory, Faculty of Sciences,
Badji Mokhtar University

Article Info

Article history:

Received 25/09/2021
Revised 16/12/2021
Accepted 19/12/2021

Keywords

Multiphase flows Industrial Problems Problems in Hydrogeology Medical Problems

ABSTRACT

Multiphase flow is of important to a variety of processes in natural and engineered porous media with complex heterogeneous features; including interactions among matters such as water, air, and oil. In fluid mechanics/dynamics, multiphase flow is simultaneous flow of materials with different states or phases (i.e. gas, liquid or solid), or materials with different chemical properties but in the same state or phase (i.e. liquid-liquid systems). A persistent theme throughout the study of multiphase flows is the need to model and predict the detailed behavior of those flows and the phenomena that they manifest. The latest developments combine a powerhouse of theoretical, ana- lytical, and numerical methods to create stronger verification and validation modeling methods. There are three ways in which such models are explored:

- experimentally, through equipped laboratory-sized models,
- theoretically, using mathematical equations,
- computationally or numerically, exploiting the power of computers to study the complexity of the flow.

Corresponding Author: *tassili.nan09@gmail.com*
Mathematical Modeling and Numerical Simulation Research Laboratory, Faculty of Sciences,Badji Mokhtar University.

1. INTRODUCTION

The multiphase flow is used to refer to any fluid flow consisting of more than one phase or component; here we exclude those circumstances in which the components are well mixed above the molecular level. This still leaves an enormous spectrum of different multiphase flows. One could classify them according to the state of the different phases or components and therefore refer to gas/solid or liquid/solid or gas/particle flows or bubbly flows, etc... Some treatises are defined in terms of a specific type of fluid flow and deal with low Reynolds number suspension flows or dusty gas dynamics. We attempt to identify the basic fluid mechanical phenomena and to illustrate them with examples from a broad range of applications and types of flow.
The general multiphase flow topologies can be identified at the outset, namely disperse flows that are consisting of finite particles, drops or bubbles distributed in a connected volume of the continuous phase; and separated flows which consist of two or more continuous streams of different fluids separated by interfaces.
This subject encompasses a vast field, a host of different technological contexts, a broad range of engineering disciplines and a multitude of different analytical approaches. The aim of the present paper is to try to bring much of this fundamental understanding and to present a unifying approach to the fundamental ideas of multiphase flows, together with different applications.

2. APPLICATION 1: GAS-OIL

We develop a simplified formulation of the hydrocarbon system used for the petroleum reservoirs simulation. This system is a model of a "system of parabolic degenerated non linear convection-diffusion" equations, which describes a two-phase flow (oil and gas) with a mass transfer in a porous medium, that leads to the fluid compressibility. Under certrain hypothesis, such as validity of Darcy's law, incompressibility of the porous medium, compressibility of the fluids, mass transfer between the oil and the gas and negligible gravity, the global pressure is formulated, due to G. Chavent, 1976 (see [5] and references therein). This formulation allows to establish theoretical results on the existence and uniqueness of the solution.

2.1. Mathematical Model

Let Ω be a bounded connected open domain of $\mathbb{R}^d$ with $d = 2$ or 3, describing the porous medium (the reservoir), with a Lipchitz boundary Γ, $t \in [0, T]$. We consider a system of PDEs of parabolic convection-diffusion type

$$\phi(x)\frac{\partial}{\partial t}(\rho_o \omega_o^h S_o) + div(\rho_o \omega_o^h U_o) = 0, \tag{1}$$

$$\phi(x)\frac{\partial}{\partial t}(\rho_g S_g + \rho_o \omega_o^l S_o) + div(\rho_g U_g + \rho_o \omega_o^l U_o) = 0, \tag{2}$$

$$U_o = -K(x)\frac{k_{ro}}{\mu_o}\nabla P_o, \tag{3}$$

$$U_g = -K(x)\frac{k_{rg}}{\mu_g}\nabla P_g, \tag{4}$$

where $S_i, U_i,\ P_i, \rho_i,\ \mu_i$ and k_{ri} denote respectively, the saturation, the velocity, the pressure, the density, the viscosity and the relative permeability of the phase $i = o\ (oil),\ g\ (gas)$, while the functions $\phi(x)$ and $K(x)$ are the porosity and the absolute permeability of the medium and ω_o^c ($c = h$ or l) is the massic fraction of component c, denoted by h for the heavy component and by l for the light one in the oil phase.
We suppose that it is a saturated regime and is expressed by

$$S_o + S_g = 1. \tag{5}$$

The capillary pressure is given by

$$P_g - P_o = P_c(S_0) = p_c(S_o)p_{cM}, \tag{6}$$

where

$$p_{cM} = \sup |P_c(S_o)|, \quad 0 \le p_c(S_o) \le 1. \tag{7}$$

We define the mobility of each phase by

$$\lambda_i = \frac{k_{ri}}{\mu_i}, \quad i = o, g \tag{8}$$

and the total mobility λ by

$$\lambda = \lambda_o + \lambda_g. \tag{9}$$

2.1.1. Reduced Saturation

For simplicity, we set

$$\rho_o^h = \rho_o \omega_o^h,\ \rho = \rho_g + \rho_o,\ b = \rho_g \lambda_g + \rho_o \lambda_o,\ \ d = \rho_g - \rho_o \tag{10}$$

Let us define by $S_{i,m}$, the residual saturation of the fluid $i = o, g$; we write

$$S_{i,m} < S_i$$

$_{i,M}$,the maximum sat

$$S_{g,M} = 1 - S_{o,m}, \quad S_{o,M} = 1 - S_{g,m} \tag{12}$$

$$S_{i,m} \leq S_i \leq S_{i,M}, \quad i = o, g \tag{13}$$

This leads to the so-called reduced saturation S set as

$$S = \frac{S_o - S_{o,m}}{1 - S_{g,m} - S_{o,m}}, \ \ 0 \leq S \leq 1. \tag{14}$$

2.1.2. Global pressure

If $S = 0$, equation (1) disappears. This is one of the main reasons for which the terminology of the **"global pressure"** was introduced to be

$$P = \frac{1}{2}\left(P_g + P_o\right) + \gamma\left(S\right) \tag{15}$$

$$\gamma\left(S\right) = \frac{1}{2}\int\limits_{S_{o,m}}^{S} \frac{\lambda_g - \lambda_o}{\lambda} p_c'\left(\xi\right) p_{cM} d\xi \tag{16}$$

The total velocity is given by: $U = U_g + U_o$ so we can write

$$\gamma(S) = \int\limits_{0}^{S} \alpha\left(\xi\right) d\xi \tag{17}$$

$$\alpha\left(S\right) = \frac{\lambda_g\left(S\right) - \lambda_o\left(S\right)}{\lambda\left(S\right)} p_c'\left(S\right) p_{cM}. \tag{18}$$

$\alpha\left(S\right)$ is the capillary diffusion.

2.1.3. Boundary and initial conditions

We suppose that the reservoir's boundary is not permeable, we write

$$\left\{ \begin{array}{c} U.\eta = 0, \ \text{ on } \ \Gamma \times (0,T), \\ \alpha(S)\nabla S = 0, \ \text{on } \ \Gamma \times (0,T), \end{array} \right. \tag{19}$$

where η denotes the normal vector. The initial conditions are set as

$$S\left(x,0\right) = S^0\left(x\right) \ \ , \ \ P\left(x,0\right) = P^0\left(x\right) \ in \ \Omega. \tag{20}$$

Therefore, we write system $((1)-(4))$ in the following form

$$\left\{ \begin{array}{c} \Phi(x)\frac{\partial}{\partial t}\left(\rho_o^h S\right) - div\left(K(x)\rho_o^h \lambda_o(S)\nabla P\right) + \\ + div\left(K(x)\rho_o^h \alpha(S)\nabla S\right) = f_1 \\ \\ \Phi(x)\frac{\partial}{\partial t}\left(\rho S\right) - div(K(x)b(S,P)\nabla P) + \\ + div\left(K(x)d\left(P\right)\alpha(S)\nabla S\right) = f_2 \\ \\ \nabla P.\eta = 0, \ \alpha(S)\nabla S = 0, \quad on \ \ \Gamma \times (0,T) \\ S\left(x,0\right) = S^0\left(x\right) \ , \ P\left(x,0\right) = P^0\left(x\right) \ \ in \ \ \Omega \end{array} \right. \tag{PB}$$

with $f_1 = -\phi(x) S_{o,m} \frac{\partial}{\partial t}\left(\rho_o^h\right)$ and $f_2 = -\phi(x)\frac{\partial}{\partial t}\left(\rho S_{o,m} + \rho_g\right)$.

We have introduced a simplified formulation of the Hydrocarbon system where the unknowns are the reduced saturation S of one of the fluids and the global pressure P. This formulation transform the system to a coupled degenerate non linear parabolic system of elliptic equations. Hence we prove the existence and uniqueness of the solution of the resulting system, details can be found in [15] and numerical results in [16].

3. HYDROGEOLOGY: SURFASIC AND UNDERGROUND FLOWS

Recently coupling surfacic and underground flows has attracted many researchers mathematically and numerically. For, we consider models coupling Navier-Stokes and Darcy equations with a numerical approach linking the dicontinous-Galerkin method [8] and [20] and the a Posteriori Error Analysis [21].
We consider our problem on a bounded domain such that

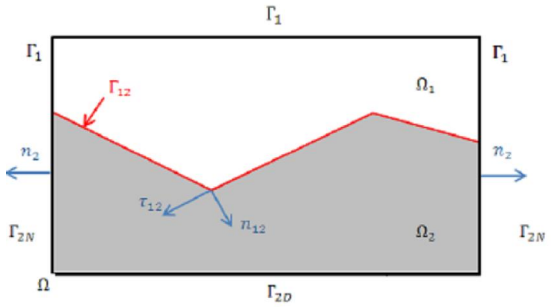

Figure 1. Coupling domain

3.1. Mathematical Model

We consider a bounded domain $\Omega = \Omega_1 \cup \Omega_2$,as in Figure 1 and write

$$\begin{cases} -\nabla.(2\nu D(u_1) - p_1 I) + u_1.\nabla u_1 = f_1 \quad \text{in } \Omega_1 \\ \nabla.u_1 = 0 \quad \text{in } \Omega_1 \\ u_1 = 0 \quad \text{on } \Gamma_1 \end{cases} \tag{21}$$

with the strain tensor $D(u_1) = \frac{1}{2}\left(\nabla u_1 + \nabla^T u_1\right)$ and a viscosity $\nu > 0$.

$$\begin{cases} -\nabla.K\nabla p_2 = f_2 \quad \text{in } \Omega_2 \\ -K\nabla p_2 = u_2 \quad \text{in } \Omega_2 \\ p_2 = g_D \quad \text{on } \Gamma_{2D} \\ K\nabla p_2.n_2 = g_N \quad \text{on } \Gamma_{2N} \end{cases} \tag{22}$$

$$\begin{cases} u_1.n_{12} = -u_2.n_{12} \\ ((-2\nu D(u_1) + p_1 I)n_{12}).n_{12} + \dfrac{1}{2}(u_1.u_1) = p_2 \\ u_1.\tau_{12} = -2\nu G(D(u_1)n_{12}).\tau_{12} \end{cases} \tag{23}$$

where u and p are the velocity and the pressure in part of the domain respectively.

The existence and uniqueness of the solution has been proved in [3].

3.1.1. Discrete Problem

To discretise ((21)-(23)), we use a finite element scheme. Let us consider a regular family of triangulations of Ω, denoted by ε^h, subdivided into elements E of diameter h, where E is a triangle in $d = 2$ or a tetrahedron in $d = 3$. We assume that all vertices of Γ_{12} and $\partial\Omega$ are vertices of ε^h and we assume that all segments of Γ_{12} are composed of segments of ε^h. For $i = 1, 2$, let ε_i^h be the restriction of ε^h to Ω_i which is also a regular family of triangulations of Ω_i. It has to be noted that the two meshes coincide at the interface Γ_{12}.
If one edge $(d = 2)$ or face $(d = 3)$ are noted by e, let Γ_i^h denote the set of edges or faces of ε_i^h interior to $\Omega_i, i = 1, 2,$. To each edge or face e of ε^h we associate once and for all a unit normal vector n_e. We set that if $e \in \Gamma_{12}$, $n_e = n_{12}$ and if $e \in \Gamma_2$, $n_e = n_2$.
We propose the discontinuous Galerkin method. For, we introduce further notation: if the function v is smooth enough, its trace along any side of one element E is well defined. If two elements E_1 and E_2 are neighbors and share one common side e, and the vector n_e points from E_1 to E_2, there are two traces of v along e. We can add or substruct those values, and we obtain a jump $[.]$ and an average $\{.\}$ for v.

The discrete problem is set as: Find $(u_1, p_1, p_2) \in X_1^h \times M_1^h \times M_2^h$ such that

$$\left\{ \begin{array}{c} \forall v_1 \in X_1^h, \forall q_2 \in M_2^h, \quad a_{\epsilon_1}(u_1, v_1) + b_{DG}(v_1, p_1) + a_{\epsilon_2}(p_2, q_2) \\ +c_{DG}(u_1; u_1, v_1) + \gamma_{12}(u_1, p_2; v_1, q_2) = L_{DG}(v_1, q_2) \\ \forall q_1 \in M_1^h, \quad b_{DG}(u_1, q_1) = 0 \end{array} \right. \tag{24}$$

with

$$\begin{aligned} a_{\epsilon_1}\left(u_1^h, v_1^h\right) &= 2\nu \sum_{E \in \varepsilon_1^h} \int_E D(u_1^h).D(v_1^h) \\ &\quad -2\nu \sum_{e \in \Gamma_1^h \cup \Gamma_1} \int_e \left\{D(u_1^h).n_e\right\} \left[v_1^h\right] \\ &\quad +2\nu\epsilon_1 \sum_{e \in \Gamma_1^h \cup \Gamma_1} \int_e \left\{D(v_1^h).n_e\right\}.\left[u_1^h\right] \\ &\quad +J^1\left(u_1^h, v_1^h\right), \end{aligned}$$

$$b_{DG}\left(v_1^h, p_1^h\right) = -\sum_{E \in \varepsilon_1^h} \int_E p_1^h \nabla.v_1^h + \sum_{e \in \Gamma_1^h \cup \Gamma_1} \int_e \left\{p_1^h.n_e\right\}.\left[v_1^h\right],$$

$$\begin{aligned} a_{\epsilon_2}\left(p_2^h, q_2^h\right) &= \sum_{E \in \varepsilon_2^h} \int_E K\nabla p_2^h.\nabla q_2^h - \sum_{e \in \Gamma_2^h \cup \Gamma_{2D}} \int_e \left\{K\nabla p_2^h.n_e\right\}.\left[q_2^h\right] \\ &\quad +\epsilon_2 \sum_{e \in \Gamma_2^h \cup \Gamma_{2D}} \int_e \left\{K\nabla q_2^h.n_e\right\}.\left[p_2^h\right] + J^2\left(p_2^h, q_2^h\right), \end{aligned}$$

$$\begin{aligned} L_{DG}\left(v_1^h, q_2^h\right) &= \int_{\Omega_1} f_1.v_1^h + \int_{\Omega_2} f_2.q_2^h + \sum_{e \in \Gamma_{2N}} \int_e g_N.q_2^h \\ &\quad +\epsilon_2 \sum_{e \in \Gamma_{2D}} \int_e \left(K\nabla q_2^h.n_e + \frac{\sigma_e^0}{|e|} q_2^h\right).g_D, \end{aligned}$$

$$\begin{aligned} c_{DG}\left(u_1^h; v_1^h, w^h\right) &= \sum_{E \in \varepsilon_1^h} \int_E \left(u_{1.}^h \nabla v_1^h\right).w^h + \frac{1}{2} \sum_{E \in \varepsilon_1^h} \int_E \nabla u_1^h.\left(v_{1.}^h w^h\right) \\ &\quad -\frac{1}{2} {}_{e \in \Gamma_1^h \cup \Gamma_1} \int_e \left(\left[u_1^h\right].n_e\right).\left\{v_1^h.w^h\right\} \\ &\quad +{}_{E \in \varepsilon_1^h} \left[\int_{\partial E \setminus \Gamma_{12}} \left\{u_1^h\right\}.n_E \left(v_1^{h(int)} - v_1^{h(ext)}\right).w^{h(int)}\right], \end{aligned}$$

and

$$\begin{aligned} \gamma_{12}\left(u_1^h, p_2^h; v_1^h, q_2^h\right) &= \left(p_2^h, v_1^h.n_{12}\right)_{\Gamma_{12}} + \frac{1}{G}\left(u_1^h.\tau_{12}, v_1^h.\tau_{12}\right)_{\Gamma_{12}} \\ &\quad -\left(u_1^h.n_{12}, q_2^h\right)_{\Gamma_{12}} - \frac{1}{2}\left(u_1^h.u_1^h, v_1^h.n_{12}\right)_{\Gamma_{12}} \end{aligned}$$

3.2. Numerical Results

We have considered a problem coupling Navier-Stokes/Darcy equations and proposed the discontinous galerkin finite element method, and we obtained local a posteriori error estimations and error indicators of a residual type [1], [7], [13] and [21]. In Figure 2, we plot the error estimates and indicators for both the continous and discontinous Galerkin approach and by comparing them, we can deduce that:

- The continous Galerkin method is more stable for this nonlinear coupled problem and takes less CPU time.
- The discontinous Galerkin method is more realistic for this type of problems.
- Error indicators are more or less of the same order.

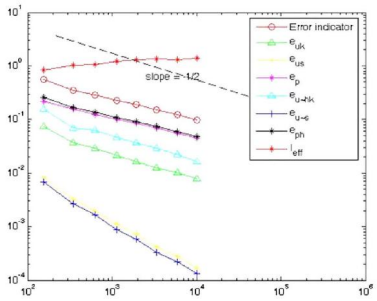

Figure 2. Error estimators and indicators

4. SURFASIC AND UNDERGROUND FLOWS IN POROUS MEDIA

4.1. Immiscible fluids

The system of equations for the flow of two immiscible fluid phases is given by the mass conservation equations combined with the Darcy's law

$$S_i \frac{\partial(\Phi_i)}{\partial t} + \nabla.(v_i) = q_i \quad i = f, s, \tag{25}$$

$$v_i = -\frac{k\rho_i g}{\mu_i}\nabla\Phi_i, \tag{26}$$

The unknowns Φ_i and v_i are the hydraulic load and the fluid velocity. The parameters S_i, k, μ_i, ρ_i and g are respectively , the storativity's coefficient, the soil permeability, the dynamic viscosity, the density and the gravitational acceleration. The position of the interface can be determined by

$$h = (1+\delta)\Phi_s - \delta\Phi_f \tag{27}$$

where $\delta = \frac{\rho_f}{\rho_s - \rho_f}$, is the density contrast beween the two fluids.

4.1.1. Simplified model

We consider a confined aquifer (Figure 3), leading to assume that the fresh water is quasi-static to give a system of partial differential equations of degenerate elliptic-parabolic type. We simplify our system by omiting the term with S_i in (25) to get

$$\alpha\frac{\partial h}{\partial t} - div(K(x)T_s(h)\nabla h) + div(K(x)T_s(h)\nabla\Phi_f) = -I_s, \quad \text{in } \Omega, \tag{28}$$

$$-div\left(K(x)H_2\nabla\Phi_f\right) + div\left(K(x)T_s(h)\nabla h\right) = I_s + I_f, \quad \text{in } \Omega, \tag{29}$$

$$h = h_D, \quad \Phi_f = \Phi_{f,D} \quad \text{on } \Gamma\times[0,T], \tag{30}$$

$$h(x,0) = h_0(x) \quad \text{in } \Omega, \tag{31}$$

where α is the porosity, $K(x)$ the hydraulic conductivity, H_2 the aquifer thickness and $T_s(h) = H_2 - h$, the salt water zone thickness. The unknowns are the hydraulic load of fresh water Φ_f and the interface depth h. the well posedness is proved in Djedaidi et al 2016 [12].

Figure 3. Confined aquifer

4.2. Finite volume approximation

In this section we propose a finite volume scheme to approximate the solutions of the derived simplified model ((28)-(31)). The time interval $[0, T[$ is divided into finite sub-intervals $[t_n, t_{n+1}]$ of length $\Delta t_n,\ n = 0, ...,\ M$ with $t_0 = 0$ and $t_M = T$. The space domain (the confined aquifer Ω) is discretized by a non-structured stitching T_h as follows.

We introduce the following notation:

- Let $|C|$ denote the cell C surface, $N(C)$ the set of triangles having in common a side with the cell C.
- Let $e_{C,L}$ be the common side of the triangles C and L, $\overrightarrow{\eta}_{C,L}$ be the normal oriented from C towards L.
- $\overrightarrow{\eta}_{e_i}$ is the external normal corresponding to the part of e_i at the boundary Γ.
- Let Q_h be the set of sides of the stitching T_h and Q_h^* be the set of the interior sides.
- For a given side e, let us denote by N and P the extremities, by W and E the two triangles where $e = \bar{W} \cap \bar{E}$; by χ_e the diamond cell associated with e given by connecting the centers of gravities of the cells W and E with the extremities N and P of e.
- $\left((\varepsilon_i)_{i=1,4}\right)$ are the four segments forming the border of χ_e.
- $\overrightarrow{\eta}_{\varepsilon} = \frac{1}{|\varepsilon_i|}(\mu_{x_i}, \mu_{y_i})$ is the normal on ε_i outgoing of χ_e.
- For a given node, $V(N)$ is the set of triangles with this node in common.

This is resumed by the more illustrative Figure 4. For more details on finite volume methods see [13].
For the numerical resolution of our simplified system ((28)-(31)), equations (28) and (29) are discretized separately.

4.2.1. Numerical Results

We explore the depth of the interface for $T = 0, 5, 10$ and 20. The numerical results are summarised in Figure 4, showing the evolution in time of the sharp interface between the fluids. Note that the interface shape is conserved.

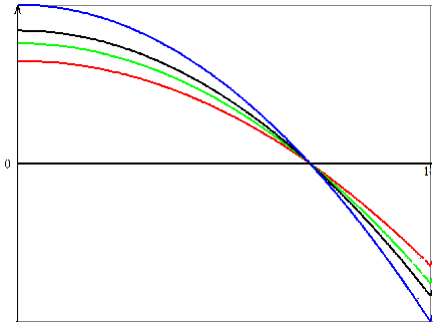

Figure 4. Depth of the interface for $T = 0, 5, 10$ and 20

4.3. Miscible Fluids

The study of miscible fluids is motivated by many applications such as oil recovery, problems in hydrogeology, groundwater pollution and fitration, where there is no sharp interface and fluids can mix freely with each other. However it is possible that two fluids or liquids are not completely miscible, i.e they can mix until the concentration reaches a certain saturation. Many authors have studied this phenomenon from different angles, for example D. Kortweg in 1901 in [17] has induced that the charge of concentration gradients near the transition zone causes capillary forces between the two fluids. The authors N. Bessov et al in [9], have pointed out that due to inohomogeneties of concentration, one should take into account the Kortweg stress. This criteria was first introduced by Kostin et al in [18], where they set their system as the incompressible Navier Stokes equations.We have also studied miscible fluids coupling concentration and Navier-Stokes equations, see Nouri et al [4].
The model that describes the movement between two miscible liquids in a porous medium, in a domain $\Omega \subset \mathbb{R}^2$ is given by the system

$$\begin{cases} \frac{\partial c}{\partial t} + u.\nabla c = d\triangle c \\ \frac{\partial u}{\partial t} + \frac{\mu}{K}u = -\nabla p + \nabla.F(c) \\ div(u) = 0 \\ \frac{\partial c}{\partial \eta} = 0,\ u.\eta = 0 \quad \text{on } \Gamma, \quad \Omega \subset \mathbb{R}^2 \\ c(x,0) = c_0(x), u(x,0) = u_0(x), \quad x \in \Omega \end{cases} \tag{32}$$

where u, p, c are the velocity, the pressure and the concentration, respectively. The coefficients d, μ and K are the mass diffusion, the viscosity and the permeability of the medium coefficients. Note that

$$\nabla.F(c) = \begin{pmatrix} \frac{\partial F_{11}}{\partial x_1} & \frac{\partial F_{12}}{\partial x_2} \\ \frac{\partial F_{21}}{\partial x_1} & \frac{\partial F_{22}}{\partial x_2} \end{pmatrix}$$

where $F_{11} = k(\frac{\partial c}{\partial x_1})$, $F_{22} = k(\frac{\partial c}{\partial x_1})$, $F_{12} = F_{21} = -k(\frac{\partial c}{\partial x_1})(\frac{\partial c}{\partial x_2})$ with k a positive constant. For more details on the study of this system the reader is referred to [1] and Assala et al in [12].

5. NUMERICAL DISCRETISATION

For the numerical resolution of the problem (32), we discretise the two first equations separately, by the finite volume scheme described in previous section. We visualise in figure 4 the concentration for different times. We conclude that the more dense fluid displaces slowly such that:

- The concentration of salt is diffusing rapidly in time.
- The velocity of water is increasing in the x-direction more than the y-direction, due to our boundary conditions assumption.
- Due to Archimedes 'buoyancy principle', the lighter fluid tend to go upward with appearance of Rayleigh–Taylor instabilities at the bottom denser layer.

In the case of immiscible fluids, the viscosity and the abrupt interface act as stabilising factors (see Djedaidi and Nouri [12] and references therein). In miscible fluids in porous media,the stabilising role of interfacial tension is played by molecular diffusion and also by a reduced density contrast, as a result of a mixing zone. Therefore, through these illustrative numerical results the classical phenomenon like merging and tip splitting, are observed.

(a) (b)

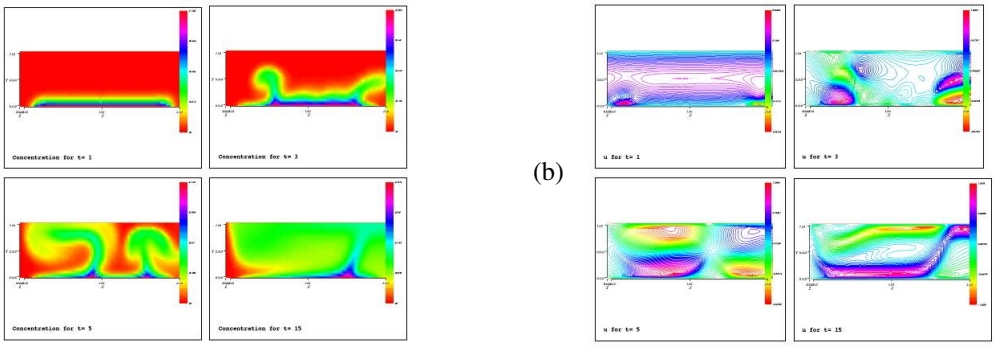

Figure 5. Concentration (a) and velocity (b) for $t = 1, 3, 5$ and 15

6. MATHEMATICS IN MEDICINE

6.1. Stem Cell Problem

The majority of orthopaedics tissues have become targets for cellular therapies, with the repair of cartilage defects, tendons and intervertebral discs. Usually such therapies introduce cells through local delivery i.e. direct injection or surgical implantation; however this method is not without limitations, for example inaccessible locations and multiple sites, the need for repeated dosage and the lack of surgical candidates.

6.2. Requirement and Suggestions

Requirement: Kyrtatos 2009, Huang et al 2010, Riegler et al 2010, Elhaj 2012 [2] wondered about the best way to:

- Deliver MSCs to their intended site(s) of action.
- Use magnetic labelling : A way to guide **MSCs** out of the bloodstream

Literature review

Richardson et al 2000 concentrated on the force experienced by the particles in a vessel due to fluid flow and the externally applied magnetic field, i.e. use Poiseuille.

Grief et al 2005 proposed an advection-diffusion model for motion of magnetic particles in the bloodstream. From these suggestions many questions arise.

Primary Questions: The primary question put to the study group was to consider whether loading MSCs with magnetic particles would enable them to be directed to specific sites, deep in the tissue with the external application of magnets.

Secondary Questions: If the approach is feasible then

1. The optimal number of Super Paramagnetic Iron Oxide particles (SPIOs) in a cell; predicting the proportion of SPIO-loaded cells that reach the target site;
2. how long MSCs take to reach the target site and

3. for what length of time external magnets should be used.

For given data by K. Elhadj and L.Kimpton 2012, the magnet against patient's skin, showing coordinate system, and the parameter values for magnetic force calculation are shown in Figure 6.
Here we visualise the spatial variation of the magnitude and direction of the force due to the magnet felt by a single core (see Figures 7), for more details on the analytical solution the reader is referred to the research report report in https://mmsg.mathmos.net/uk/2012/magnetic-stem-cells/report.pdf . The key things to note are that the force is always directed towards the magnet and that the magnitude of the force decays rapidly away from the magnet.

(a)

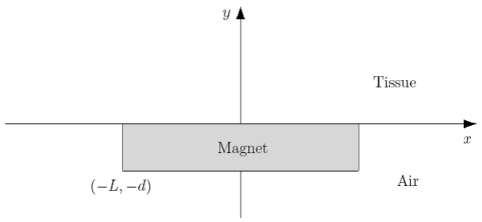

(b)

Parameter	Value	Units
ρ	5.1×10^{3}	kgm^{-3}
M_{sat}	50	$\mathrm{Am}^{2}\mathrm{kg}^{-1}$
r_{core}	5×10^{-9}	m
k	1.38×10^{-23}	$\mathrm{m}^{2}\mathrm{kgs}^{-2}\mathrm{K}^{-1}$
T	310	K
d	2×10^{-3}	m
L	3.5×10^{-3}	m

Figure 6. Coordinate system (a), and the parameter values (b) for magnetic force calculation.

(a)

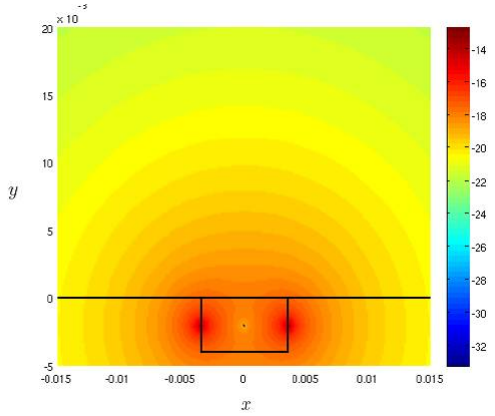

(b)

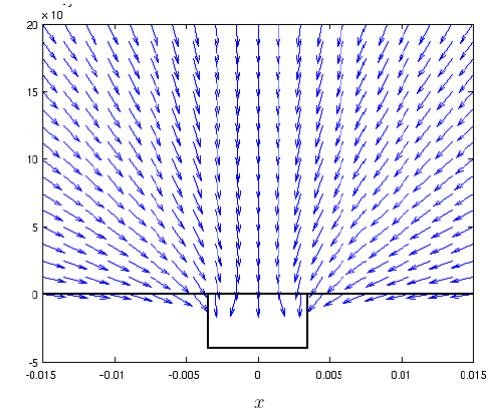

Figure 7. Magnitude of the force (a), and its direction (b) due to the magnet felt by a single core.

6.3. Proposed Model

First sight: We propose a model taking into account the following two reactions:
* The action of the fluid on the cell is modelled by the hydrodynamic force and torque acting on its surface, they are used as the right-hand sides of Newton-Euler equations.
* The action of the cell on the fluid can be modelled by no-slip boundary conditions on the cell in the Navier–Stokes equations.

Inconvenience of this Model
This explicit coupling can be numerically unstable and its resolution often requires very small time steps. In addition, if we choose to use (for accuracy) the finite element menthod and since the position of the cell evolves in time, we would have to remesh the computational domain at each time step or in best cases every few time steps.

6.3.1. Bi-Phasic Model (Fluid-Bubble)

We propose a bi-phasic model assuming that we have two fluids with different densities and viscosities, using Navier Stokes equations

$$\rho(\phi(x,t))\partial_t u + \rho(\phi(x,t))(u.\nabla u) - \mu(\phi(x,t))\Delta u + \nabla p = f \ , \tag{33}$$

with

$$\rho(x,t) = \begin{cases} \rho_f & \forall x \in \Omega_f \\ \rho_b & \forall x \in \Omega_b \end{cases} \ , \ \mu(x,t) = \begin{cases} \mu_f & \forall x \in \Omega_f \\ \mu_b & \forall x \in \Omega_b \end{cases} \tag{34}$$

and

$$\rho(\phi) = \rho_b + (\rho_f - \rho_b)H(\phi) \ , \ \mu(\phi) = \mu_b + (\mu_f - \mu_b)H(\phi) \tag{35}$$

and the level set method. Here $H(\phi)$ denotes the Heaviside function and $\phi(x,t)$ is the level set function defined by

$$\begin{cases} \phi(x,t) > 0 & \forall x \in \Omega_f \\ \phi(x,t) < 0 & \forall x \in \Omega_b \\ \phi(x,t) = 0 & \forall x \in \Gamma \end{cases} \tag{36}$$

The evolution of the interface Γ at each time t is described by the advection of the level set function $\phi(x,t)$ solution of

$$\begin{cases} \partial_t \phi + u \ \nabla \phi = 0 & \forall x \in \Omega \times (0,T) \\ \phi = \phi_{in} & on \ \ \Sigma_{in} \\ \phi = \phi_0 & \forall x \in \Omega \ at \ t = 0 \end{cases} \tag{37}$$

where $\Sigma_{in} = \{(x,t) \in \partial\Omega \times (0,T); \ u.n < 0\}$. We introduce a relaxation parameter λ $(0 \leq \lambda \leq 1)$ such that $u = \lambda u_f + (1-\lambda)u_b$, and we use

$$H(\phi) = \begin{cases} 0 & if \quad \frac{\phi}{|\nabla\phi|} < -\varepsilon \\ \frac{1}{2}(1 + \frac{1}{\varepsilon}\frac{\phi}{|\nabla\phi|} + \frac{1}{\pi}\sin(\frac{\pi}{\varepsilon}\frac{\phi}{|\nabla\phi|})) & if \quad -\varepsilon \leq \frac{\phi}{|\nabla\phi|} \leq \varepsilon \\ 1 & if \quad \frac{\phi}{|\nabla\phi|} > \varepsilon \end{cases} \tag{38}$$

where $[-\varepsilon, \varepsilon]$ is the thickness of the interface between the fluid and the cell. Note that the heaviside function $\mathbf{H}(\phi)$ does not depend on ϕ but on $\frac{\phi}{|\nabla\phi|}$ as an approximation of the distance function in the neighbourhood of the interface.

6.4. Numerical Results

In this section we present some numerical solutions for a simple model of a cell in a blood vessel in the presence of a magnetic eld. The position and deformation of the cell not only depends on the interaction between the flow and the cell, which are quite complex in such a geometry, but also on the initial position of the cell(s).
In the same way as in the previous applications, we use a finite element scheme to solve ((33)-(38)) using the following algorithm.

Input f (Magnetic Field force) and the disctretisation parameters
Update $\rho(\phi)$ and $\mu(\phi)$
Solve the Navier Stokes equation (33)
Use the velocity u of Navier Stokes Equation to advect ϕ from (37),

and get the following results:

Case 1. Low Magnet Effect, $\lambda = 0.35$, it is clearly shown in Figure 8 that the cell is pushed straight to the end of the domain by the blood and slightly pulled down in the middle part of the domain by the magnet.

Case 2. High Magnet Effect, $\lambda = 0.85$, as shown in Figure 9, we can notice that in addition to the the blood effect pushing, the magnet is pulling the cell.

Case 3. Two Cells with low Magnet Effect, $\lambda = 0.35$, in this last numerical experiment we noticed numerical unstable behaviour, the two cells are pushing each other in addition to the blood effect and the cell motion, as shown in Figure 10.

The numerical results in this section prove a possible framework for numerical simulations of cell motion through the bloodstream in the presence of a magnet (see Figures 8,9 and 10). The interface Γbetween cell and blood is clearly seen to diffuse at some of the later time points and there is some pinching of the cell under the influence of strong magnets (see Figure 9). Modelling could be useful in determining how strong a magnetic force would need to be to have a sufficient effect on this process. Another interesting problem concerns how loading cells with magnetic particles in instigates their strolling motion.

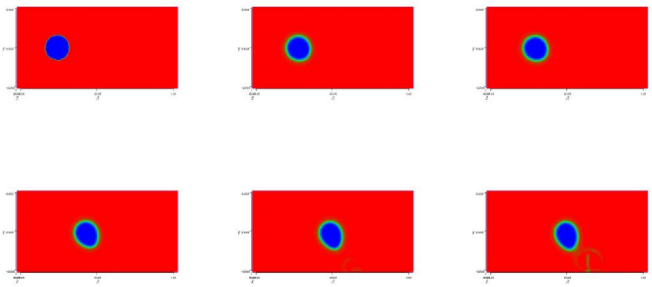

Figure 8. Low Magnet Effect for one cell, $\lambda = 0.35$

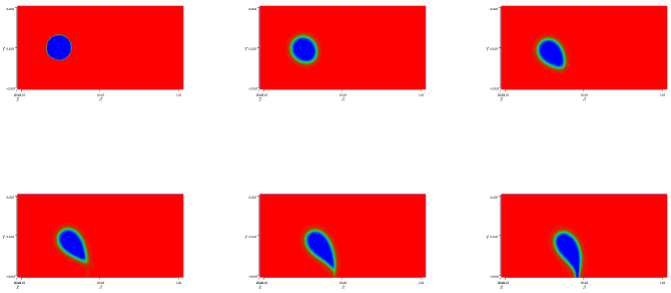

Figure 9. High Magnet Effect for one cell, $\lambda = 0.35$

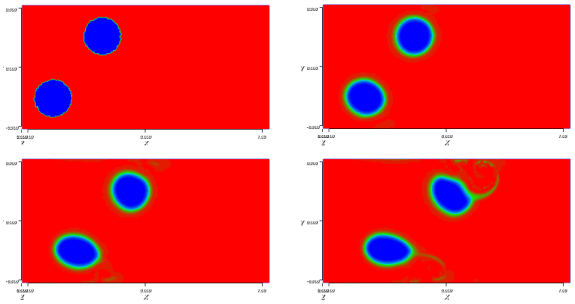

Figure 10. Low Magnet Effect for two cells, $\lambda = 0.35$

7. CONCLUSION

Through these different applications, we show how mathematical modelling can be of a great use. By studying a real problem, we first learn new skilsl and try to seek and develop new methods and approaches leading to solutions in a record time, helping experimentalists to understand complex phenomena.
We can also refer to [6] for some userful results solving a real problem in cardiology and [10] for a problem in pharmacolgy.

AcknowledgementI am very grateful to the mathematics in medecine and in industry UK-Networks which bring researchers from different fields to work together on a specific real problem; giving opprotunities to learn from each other new skills.

REFERENCES

[1] A. Agouzal, A posteriori Error Estimates for non conforming approximations, Int. J. Numer. Anal. Modeling, 5(1): 77-85, (2008).
[2] M. Albert-Gimeno, I. Hadji, T. Joshi, L. Kimpton, T. Kwan, G. Lang, S. Moise, S. Naire, F. Nouri, G. Richardson, R. Whittaker, Targeting stem cells following I.V. injection using magnetic particle based approaches, https://mmsg.mathmos.net/uk/2012/magnetic-stem-cells/report.pdf, pp. 1-16, 2012
[3] A Study of a Problem Coupling Surfacic and Underground Flows, Int. Journal of Math. Analysis, Vol. 7, 2013, no. 50, pp.2475 - 2489.
[4] A. Assala, N. Djedaidi and F.Z. NouriDynamical behaviour of miscibles fluids in porous media, International Journal of Dynamical Systems and Differential Equations Vol. 8(03), DOI:10.1504/IJDSDE.2018.10009554, 2018, pp. 190-203.
[5] L. Badea, M. Discacciati & A, Quarteroni. Mathematical analysis of the Navier-Stokes-Darcy coupling, Numerische Mathematik, 2010, Vol 115, Issue 2, pp. 195-227.
[6] CG Bell, K Bentahar, EC Chang, AJE Foss, LD Hazelwood, HD Holm, Z Jones, S Naire, FZ Nouri, JC O'Flaherty, NS Peters, CP Please, SF Pravdin, G Richardson, A Setchi, RJ Shipley, JH Siggers, MJ Tindall, JP Ward, Mechanisms and localised treatment for complex heart rhythm disturbances, https://mmsg.mathmos.net/uk/2009/heart-rhythm/report.pdf, pp.1-22.
[7] C. Bernardi, F. Hecht & F.Z. Nouri. A New finite element discretisation for the solution of Stokes problem coupled with Darcy equation, IMA J. Numerical Analysis, 2010, Vol 30, pp.61-93.
[8] C. Bernardi, Y. Maday & F. Rapetti. Discrétisations variationnelles de problèmes aux limites elliptiques, Springer Verlag Berlin Heidenberg, Mathématiques et Applications 45, 2004.
[9] Bessonov, N., Volpert, V.A., Pojman, J.A. and Zoltowski, B.D. (2005) 'Numerical simulations of convection induced by Korteweg stresses in miscible polymermonomer systems', Microgravity Science and Technology, Vol. 17, pp.8–12.
[10] Bram G. Sengers, Sean McGinty, Fatma Z. Nouri, Maryam Argungu, Emma Hawkins, Aymen Hadji, Andrew Weber, Adam Taylor & Armin Sepp, Modeling bispecific monoclonal antibody interaction with two cell membrane targets indicates the importance of surface diffusion, mAbs, 8:5, DOI:10.1080/19420862.2016.1178437, 2016, pp.905-915.
[11] M. Discacciati, A, Quarteroni. Navier-Stokes-Darcy coupling : Modeling, Analysis and numerical approximation, Rev. Mat. Complut, 2009, Vol 22(2), pp. 315-426.
[12] N. Djedaidi, F. Z. Nouri, A study for flow interactions in heterogeneous porous media, Comm. in Optimistion Therory, Article ID 8 (7 June 2016), pp.1-11.
[13] M.L. Hadji, A. Assala and F.Z. Nouri, A posteriori error analysis for Navier–Stokes equations coupled with Darcy problem, Calcolo, Issue 4/2015, pp. 559-576.
[14] F. Hecht, O. Pironneau. FreeFem++, see www.freefem.org.
[15] S. Gasmi and FZ Nouri,
[16] S. Gasmi and F.Z. Nouri, Numerical simulation for two-phase flow in a porous medium, Gasmi and Nouri Boundary Value Problems (2015) 2015:7 DOI 10.1186/s13661-014-0256-6.
[17] Korteweg, D. (1901) 'Sur la forme que prennent les équations du mouvement des fluides si l'on tient compte des forces capillaires causées par des variations de densité ', Archives Neerlandaises des Sciences Exactes et Naturelles, Series II, Vol. 6, pp.1–24.
[18] Kostin, I., Marion, M., Picar, R.T. and Volpertd, V.A. (2003) 'Modelling of miscible liquids with theKorteweg stress', Mathematical Modelling and Numerical Analysis, Vol. 37, No. 5, pp.741–753
[19] F.Z. Nouri, A New Approach for a Multiphase Flow Problem, Int. of Maths and Computation, 2019 Volume 30, Issue Number 3, 2019, pp.32-45.
[20] B. Rivière, Discontinuous Galerkin Methods for Solving Elliptic and Parabolic Equations, Theory and Implementation, Frontiers in Applied Mathematics, 2008
[21] R. Verfuth , A Posteriori Error Estimation techniques for F.E.M., Oxford Science publications 2013.

BIOGRAPHIES OF AUTHORS

Fatma Zohra Nouri is a professor in the department of mathematics, with a Msc (1985) and Phd (1988) from Oxford-Strathclyde-UK university. She is the director the Mathematical Modeling and Numerical Simulation Research Laboratory.
Her researches are in fields of Applied Mathematics, Fluid Mechanics, Mathematical modeling and Numerical Analysis & Simulations. For the last two decades she has been involved in studing problems issued from industry, medical sciences and Plant Sciences
She is the vice president of the Algerian Mathematical Society and reviewer in differents Applied Mathematics journals.
Further info on her homepage: http://lam2sin.univ-annaba.dz/